Crystallization in Thin Liquid Films Induced by Shear

Mustafa Akbulut, Nianhuan Chen, Nobuo Maeda,[†] Jacob Israelachvili,* Torsten Grunewald,[‡] and Christiane A. Helm[‡]

Departments of Chemical Engineering and Materials and the Materials Research Laboratory, University of California, Santa Barbara, California 93106, Department of Applied Mathematics, Research School of Physical Sciences and Engineering, Australian National University, Canberra ACT 0200, Australia, and Institute of Physical Chemistry, University of Mainz, 17487 Greifswald, Germany

Received: November 11, 2004; In Final Form: March 5, 2005

It is known that the thin-film structure of confined fluids and solids can be changed when the confining surfaces are sheared. Positional and orientational short- or long-range reordering can occur that often have no bulk counterparts. These multilayer, monolayer, or even sub-monolayer effects are important for understanding adhesion and friction processes, but they have proved difficult to measure, partly due to a lack of experimental techniques and partly to their apparent subtle dependence on many experimental parameters. Here we report the use of shear measurements and "optical absorption spectroscopy" in the surface forces apparatus to measure a shear-induced phase transition of an anisotropic (dye) molecule confined between two shearing mica surfaces in aqueous solution. Our studies on the shear-induced ordering and friction forces of highly anisotropic cyanine dye molecules in thin water films show only a weak effect of molecular anisotropy on shear-induced ordering, friction forces, and the onset of shear-induced crystallization, although dramatic changes do occur when the confined molecules ultimately crystallize.

Introduction

Recent measurements using the surface forces apparatus (SFA) have shown that both the normal and lateral (shear, frictional, and lubrication) forces between surfaces in liquids can be modified during shear due to changes in the structure of the confined liquid. These changes can take a long time or involve large strains before steady-state conditions are achieved. In the case of lubrication forces, these can increase (shear thickening) or decrease (shear thinning) *continuously*, sometimes by more than an order of magnitude, after the start of sliding.[1] In other cases, *discontinuous* changes are observed between high and low friction regimes (stick-slip friction) that have been theorized to represent periodic solid−liquid phase transitions of the film during sliding.[2] It is imperative to understand how these forces are related to, or determined by, changes in the ordering of the liquid molecules, which may involve both positional and orientational ordering over a short (local clustering) or long (ordered domains) range and which could depend on the lattices' incommensurability, the "twist angle" between the two commensurable lattices, the shearing direction relative to these axes, the load, sliding velocity, etc.

It has been technically challenging to detect molecular alignment in nano-thin-films in situ because of the minute sample size and the likely transient or fluctuating nature of the changes. One promising approach, which was proposed and tested some years ago,[3] is to use a molecular probe such as a light-absorbing dye in the narrow gap between the two mica surfaces usually used in the SFA. Even though the amount of the dye in the gap may be less than a monolayer, the absorption is enhanced due to the multiple reflections and passes of the light through the film when it is visualized using the multiple-beam interference fringes (known as fringes of equal chromatic order or FECO). The multiple reflections occur between the silver layers deposited on the backsides of the mica sheets. The electric field of the light in the middle of the interferometer, i.e., where the confined film is located, is effectively zero for the "even-order" fringes and maximum for the "odd-order" fringes. When the confined layer is much thinner than the thickness of the mica sheets, there is a marked contrast in the intensity between the even (absorbing) and odd (nonabsorbing) fringes, which can be readily seen and recorded.

In principle, the difference or ratio of odd-to-even order intensities, its dependence on the two birefringent components of the FECO fringes, and the wavelength at which the absorption is maximum can provide information on the concentration of trapped/confined dye molecules, the direction at which they are oriented/aligned in the film (if the molecule is asymmetric, e.g., linear), and the local temperature or pressure (if the absorption spectrum of the dye is temperature or pressure sensitive).

For our studies, we have chosen the water-soluble anisotropic cationic polymethine dye molecule, cyanine (Figure 1a), which adsorbs to the negatively charged surface of mica in solution and can therefore be trapped between two mica surfaces when these are brought together. The absorption spectrum of polymethine, including the shape and peaks of the spectral envelope, depends on its state, i.e., whether fully dissolved or aggregated in solution, in a thin film, on a surface, or in the crystalline form.[4] Polymethine dyes are used for a variety of purposes such as photoreceptors in certain photophysical and photochemical processes, photoactive materials and saturable absorbers in dye lasers and solid-state diode lasers, as probes of membrane potential and mobility, and as inhibitors of rapid cell growth.[5]

In aqueous solutions, they tend to form aggregates consisting of tightly packed molecules with their molecular planes stacked against each other.[6] When adsorbed to a mica surface, the molecular planes are assumed to be at right angles to the mica

* To whom correspondence may be addressed. E-mail: jacob@engineering.ucsb.edu.
[†] Australian National University.
[‡] University of Mainz.

10.1021/jp0448200 CCC: $30.25
Published on Web 06/02/2005

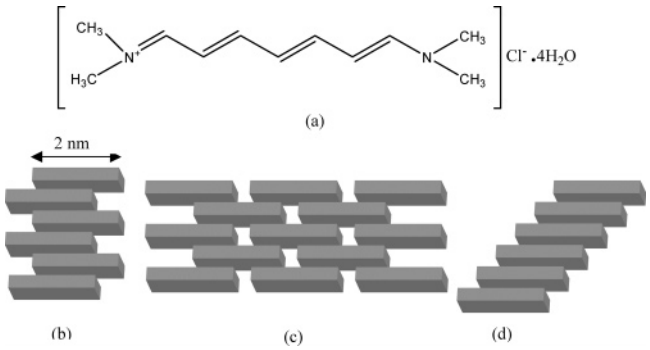

Figure 1. (a) Molecular formula of the polymethine cyanine dye, BDH^+Cl^-, used in these experiments. Three different possible arrangements of the dye molecules on mica surfaces: (b) ladder arrangement, (c) brickstone arrangement, and (d) staircase arrangement.

surface as the positively charged N^+ atoms of the molecules fill the negative holes left by the dissociation of the K^+ ions.[7] Three different arrangements of the adsorbed dye molecules on mica are possible,[7] known as the brickstone, ladder, and staircase arrangements, illustrated in parts b, c, and d of Figure 1.

Experimental Section

1,7-Bis(dimethylamino)heptamethine chloride (BDH^+Cl^-) is a water-soluble cyanine dye that has a linear structure as shown in Figure 1a. In bulk aqueous solution, the absorption spectrum has a maximum around $\lambda_{max} = 490$ nm with a half width of about 50 nm.[8] The absorption is largest for light that is polarized parallel to the long molecular axis and smallest when it is perpendicular to it. This anisotropy makes BDH^+Cl^- a potentially ideal molecular probe for studying molecular alignment in thin films (in contrast to Rhodamine B, for example, which has a high absorption coefficient (and therefore high sensitivity) but which is too isotropic in shape to be a useful probe of molecular alignment or *orientational* ordering (in contrast to *positional* ordering, this can arise for molecules of any shape)). Similar experiments to those reported here but using Rhodamine B are reported in ref 9.

To optimize the conditions for initiating and observing shear-induced molecular alignment, we prepared our mica substrates in a special way as described in ref 10. Mica has two optic axes, one of which is perpendicular to the cleavage plane. The direction of the other optic axis can be measured using a pair of polarizers prior to cleaving the mica. Once the direction of the optic axis is measured, the mica piece is cleaved and then melt-cut in such a way that the optic axis is parallel to one of the melt-cut edges. After deposition of silver on the backsides of the cleaved pieces, the mica sheets are mounted into the SFA so that the optic axes of the two surfaces are parallel to each other (the "twist angle" is zero and the two lattices are "commensurate"), and are either parallel or perpendicular to the sliding direction. In this way, the two FECO fringes for each interference order have the maximum spacing (doublet splitting) between the two birefringent components, usually referred to as the β and γ fringes or components, where $\lambda_\gamma > \lambda_\beta$. The β- or γ-fringes give the interference spectrum for light polarized parallel or perpendicular to the sliding direction depending on how the surfaces are mounted in each experiment.

In each experiment, we measured which of the β or γ components is parallel to the sliding direction by placing a polarizer below the bottom (entrance) window of the SFA and allowing only the light of known polarization to enter the two-surface interferometer. We also verified that none of the optic components along the optic path (between the light source and the spectrometer) rotates the polarization of the light.

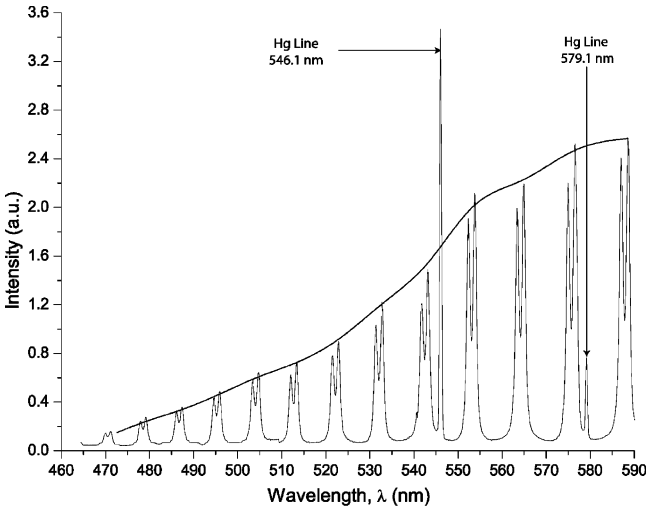

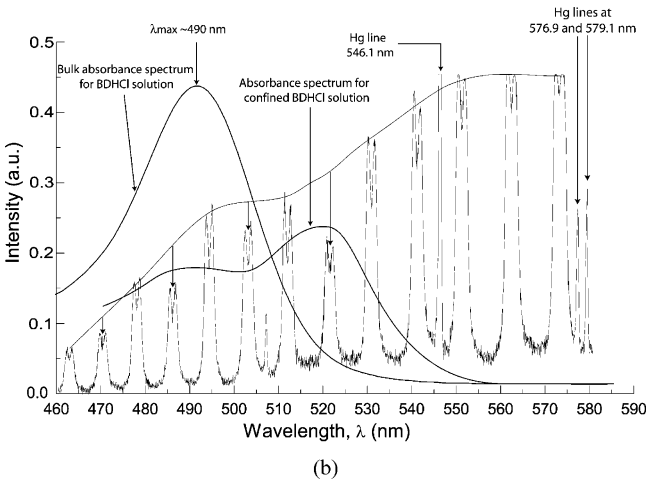

Figure 2. (a) Typical FECO intensity spectra for two mica sheets of equal thickness pressed into flattened contact with no absorbing dye layer between them. (b) The intensity spectrum when there is a film of BDH^+Cl^- of thickness $T = 15$ nm between two mica surfaces. The bulk absorption spectrum is also shown for a 10^{-3} M BDH^+Cl^- solution in pure water.

A charge-couple device camera (Roper Scientific & KDK 1037 × 1357) was used to record the FECO fringes. The cumulative error in the intensity from the recordings and image analysis was typically 6%. Thus, alignment of more than 12% of the dye molecules, either parallel or perpendicular to the sliding direction, was necessary for a measurably significant difference to arise between the intensities of the β and γ components of the even-order fringes (these being the fringes that absorb the light).

When a concentrated (approximately 1 wt %) BDHCl solution is introduced between the mica surfaces, the odd- and even-order FECO fringes within the absorption band are affected differently: the intensities of the even-order fringes are reduced, while those of the odd-order fringes remain unchanged (There is usually at least one even-order fringe within the absorption band. For thicker mica sheets (>3 μm) there are more fringes, but the accuracy of measuring the film thickness falls.) (see parts a and b of Figure 2 which correspond to the full FECO intensity spectra of fringes such as these shown in parts a and b of Figure 3). (The SFA community has traditionally referred to the fringes with nodes at the center as "odd" and with antinodes as "even". As pointed out by Briscoe et al.[11] and Heuberger et al.,[12] this designation should be reversed. In this

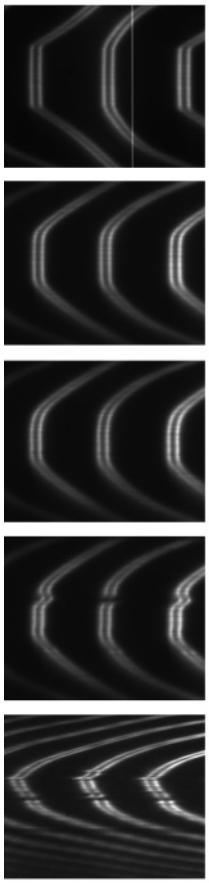

Figure 3. Example of five FECO spectra (odd−even−odd) within the absorption region of BDH^+Cl^- dye (wavelength range: 450−550 nm) for thin films of aqueous BDH^+Cl^- solutions between two mica surfaces in the SFA. The images are shown (a) before introducing BDH^+Cl^- solution between the surfaces, (b) after introducing the BDH^+Cl^- solution but before sliding of the mica surfaces, (c) during sliding at $v = 220$ nm/s but before crystallization takes place, and (d) immediately after crystallization. The crystallization shown in part d occurred near the edge of the contact zone. (e) After damage. In the first three panels a−c, the surfaces were pressed into flattened contact over a diameter of about 90 μm.

paper, we use the "correct" designations for odd-order and even-order fringes.) Comparison of the odd-to-even intensities therefore gives the amount of absorbing material between the surfaces, while the shapes of the envelopes give information on the effects of confinement or shearing. In addition, any preferred alignment of the dye molecules can be measured by comparing the intensities of the β and γ components of any even-order fringe.[11,12]

Prior to the shear experiments, a large reservoir of water was placed at the bottom of the SFA chamber to prevent evaporation of water from the droplet, which could lead to an increased concentration of the solution between the surfaces and ultimately to crystallization of the dye.

The SFA was equipped with a piezoelectric bimorph slider that slides one mica surface against the other; semiconductor strain gauges on the springs supporting the other surface were used to measure the tangential (friction) forces acting on that surface. The input voltage of the piezoelectric bimorph was supplied by a function generator (HP 3325B, Hewlett-Packard), usually using a triangular wave to slide the surface back and forth at a constant velocity.

Results

The thicknesses T of the trapped cyanine-rich films studied in the SFA were typically between 10 and 20 nm, and over this range of thicknesses the results presented below were independent of T. The refractive index of the films was also measured in situ using the standard three-layer interferometer equation[13] and found to be typically $n = 1.52 \pm 0.01$. We also measured the refractive index of a thin crystalline layer of BDH^+Cl^- using ellipsometry. Here a 1% solution of BDH^+Cl^- was cast onto a clean silicon wafer and slowly dried. Slow drying resulted in a crystalline layer typically 30 nm thick and of refractive index $n = 1.63 \pm 0.01$. Given that the refractive index of water is $n = 1.33$, the volume fraction of the cyanine molecules in our films was therefore approximately $(1.52 - 1.33)/(1.63 - 1.33) = 0.63$, which is ~60 times more concentrated than in the bulk solution.

When the mica surfaces are slid across each other with a film of BDH^+Cl^- solution between them, the kinetic friction is initially smooth and constant, and the fringes show no sign of change during the transition from rest to sliding nor during sliding: the film thickness (resolution $\approx$ 0.4 nm) and contact diameter (resolution $\approx$ 1 μm) do not change and, within our measuring accuracy, neither does the intensity of any of the fringes. This suggests no major change in the configuration of the dye molecules when the film is sheared.

However, after a certain sliding time (or sliding distance of the order of many hundreds of microns), some dye is observed to crystallize inside the contact area (see parts c and d of Figure 3), and if the surfaces are kept sliding, the newly nucleated solid crystal damages the surfaces (Figure 3e). In Figure 3d, both the components of the even-order fringes have disappeared, indicating that the absorption has increased dramatically on crystallization but also that the polarization of the absorbed light is not oriented uniquely along one of the optic axes of mica nor along the sliding direction. The absorption could be at an angle to these directions and/or at random if the nucleate consists of randomly oriented polycrystalline grains.

Another example of a shear-induced crystallization, but this time near the center of the contact zone, is shown by the FECO spectrum in Figure 4a. Intensity spectra were recorded in different regions of the contact and compared. Figure 4b shows the spectrum taken across the central crystallized region of the film. The main features are the same as those of Figure 3d but are now shown in greater detail and over a larger spectral range. The crystal of Figure 4a was thinner than that of Figure 3d so that the even fringes were not totally obliterated by the high absorption, allowing for quantitative comparisons to be made between the odd- and even-order intensities at different wavelengths. Analysis of the intensity spectrum (Figure 4b) reveals that the even-order fringes show a dark region at the center of the contact zone only for a limited wavelength range between 500 and 560 nm, peaking at $\lambda_{max} \approx 530-550$ nm, compared to $\lambda_{max} \approx 490$ nm in bulk solution and $\lambda_{max} \approx 520$ nm in confined (and concentrated as calculated above) solutions (Figure 2b). Note that the (relative) heights of the peaks are in arbitrary units for each spectrum; the absolute intensity is much higher for the crystals (Figure 4b) than for the confined solutions (Figure 2b), which in turn is much higher than for the bulk solution (also Figure 2b). The spectrum of the confined solutions appears like a superposition of two spectra: that of bulk solution and that of crystal. It is conceivable that the very high concentration of the dye in the confined solution estimated above is a result of strong adsorption of the dye molecules at the mica walls, which could have epitaxial crystalline features, sandwiching a thin layer of bulk solution in between. Furthermore, when the refractive indices of the dark (crystallized) and adjacent bright (noncrystallized) regions in Figure 4a are analyzed, one finds a

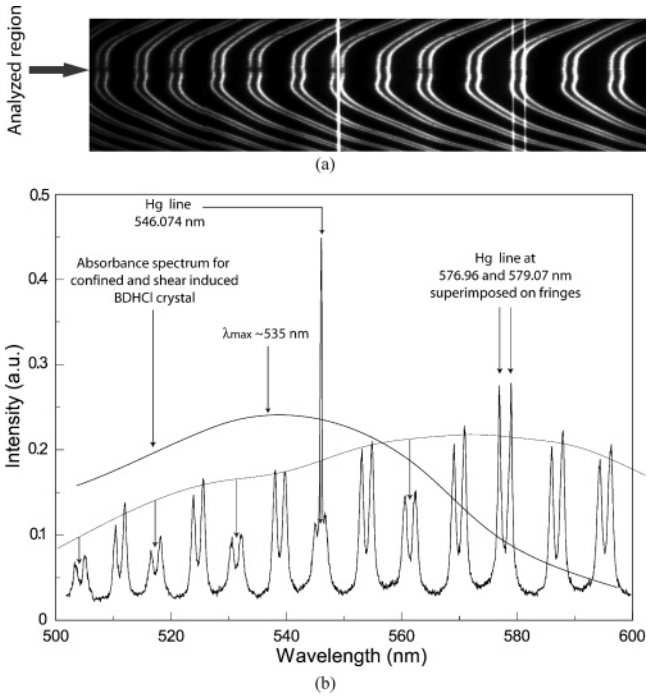

Figure 4. Example of a FECO image (a) and the corresponding spectrum (b) of a shear-induced crystal of BDH^+Cl^-. The spectrum is averaged over the cross section of where there is a discontinuity in some of the even-order fringes. The odd-order fringes remain unaffected by the presence of the crystal at all the wavelengths shown. In contrast, the even-order fringes show a discontinuity at the center of the contact zone in the wavelength range 500−560 nm but not at higher wavelengths. The strong absorption in the wavelength range 500−560 nm suggests the formation of a BDH^+Cl^- crystal.

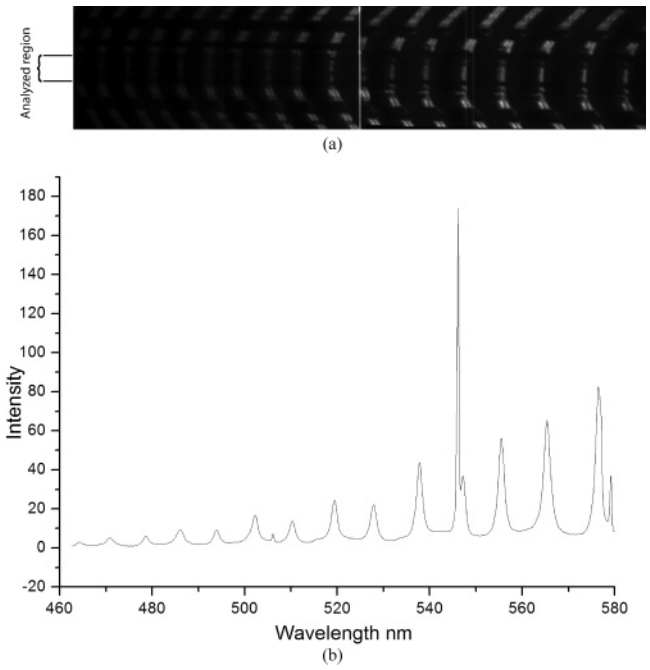

Figure 5. (a) Example of a FECO image that shows the contrast between the components due to epitaxial crystallization. (b) The corresponding spectrum (up to 580 nm) sampling the cross section indicated in part a. Prior to bringing the surfaces together, they were dried while well separated at a distance of ~500 μm (0.5 mm).

significantly higher refractive index for the 10 nm thick crystallized film of $n_\beta = 2.1 \pm 0.2$ and $n_\gamma = 1.5 \pm 0.2$ compared to that of the isotropic dye film (concentrated but noncrystallized solution) of $n = 1.4 \pm 0.2$. Thus, the refractive index of the crystallized region is birefringent, with one component, presumably along the molecules (there are no literature values for the birefringement indices of crystalline BDH^+Cl^- in any of its different configurations (shown in Figure 1) for us to compare our values with), much larger than that of the surrounding partially dried residue or concentrated solution. These features can be attributed to the higher density, increased conjugation, and anisotropy of the crystallized dye molecules.

The lack of absorption of the even-order fringes at higher wavelengths (seen also in Figure 2b), and depletion of intensity of both β and γ components by almost identical amounts within the absorption band, is consistent with randomly oriented polycrystals but also, based on the high birefringence mentioned above, with a single crystal where the absorptions along the different crystal axes are similar. These crystals, once formed, do not redissolve after the shearing of the surfaces is stopped and even after the surfaces are separated. However, the crystals could be removed by taking the surfaces out of the SFA and rinsing them thoroughly with water.

To gain further insights into this phenomenon, we investigated how the crystallization depends on the film thickness, sliding speed, the concentration of dye in the film, epitaxial effects such as the surface lattice structure, and other possibly relevant experimental parameters.

We first verified that evaporation of the solvent (water) was negligible within the time scale of each experiment; thus, the observed crystallization cannot be attributed to a bulk phase separation brought about by an increased concentration of dye in the solvent. We also found that coating the mica surfaces with layers of the polymers poly-L-lysine and polyvinyl benzyl chloride does not improve the contrast between the components of the even-order FECO fringes within the BDH^+Cl^- absorption band even at the fastest sliding speed studied ($v \approx 2.2$ μm/s). However, these polymers delay the crystallization of BDH^+Cl^- and the onset of damage up to a few hours (corresponding to the total sliding distance of a few centimeters), especially in the case of low shearing speeds ($v < 0.2$ μm/s). Still, crystallization eventually occurred, which was followed by damage of the surfaces if the surfaces are kept sliding. The delayed crystallization between the polymer-coated surfaces may be explained as being due to the softness and nonuniformity of polymer layer, allowing for patches of the mica surfaces to become exposed to the dye or to the dye penetrating through the layers.

We also studied the effect of the film thickness on the nucleation and crystallization: prolonged shearing of the surfaces at larger separations of $T \approx 200$ nm never resulted in crystallization or damage.

When the surfaces were intentionally dried, very different features emerged. After the BDH^+Cl^- solution is dried while the surfaces are kept in contact in the SFA, the surfaces exhibit unmeasurably high static friction, i.e., they become totally stuck. Presumably the positively charged dye molecules sandwiched between two negatively charged mica surfaces cause strong electrostatic binding between the mica surfaces. It appears that these crystals are different from those that occur during sliding when the surfaces do not get stuck (see Figures 3). It is worth noting that the drying still leads to the formation of a smooth film of dye between the mica surfaces. This is not the case if the surfaces are dried when separated, which generally resulted in rough surfaces (see, for example, Figure 5).

When the mica surfaces are kept separated by about 500 μm and the dye solution between the surfaces is allowed to slowly evaporate (over 12 h), BDH^+Cl^- forms a thick crystalline layer

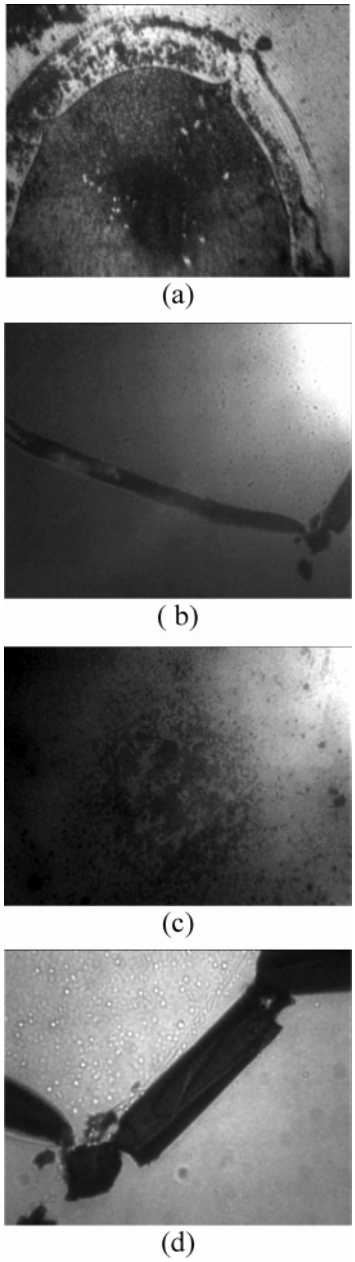

Figure 6. Images of BDH^+Cl^- multilayers obtained using an optical microscope (Nikon, Eclipse E) with $\times 50$ magnification in transmission mode. (a) Former contact region after mica surfaces were dried while the surfaces were kept in contact. (b) The same as in part a but outside the former contact region. There are a number of similar crystals outside in the former contact region. (c) Center region after the mica surfaces were dried while separated by a large distance. (d) The same as in part c but outside the center region. There are a number of similar crystals in the off-center region.

on one or both surfaces which, on one occasion, resulted in the complete disappearance of the β, but not the γ, component as shown in Figure 5. Here, no contrast in the intensities between the *visible* odd- and even-order fringes is observed, suggesting that the crystal layer thus formed is very thick (at least comparable to that of the mica sheets). The absence of the β component is a result of very strong absorption of the light polarized parallel to the β axis, suggesting that many dye molecules are aligned parallel to the β axis. The clear presence of the gamma component, on the other hand, shows that there are hardly any BDH^+Cl^- molecules aligned parallel to the γ axis. Given that the β axis is almost perpendicular to the γ axis, it is reasonable to conclude that BDH^+Cl^- molecules are almost exclusively aligned parallel to the β axis as they crystallize by slow drying. These results suggest that slow drying of the dye solution may grow a large single crystal epitaxially on the mica lattice. Unfortunately, these surfaces are not smooth enough for sliding or friction measurements that can be compared to those of initially smooth surfaces. So all this suggests that some crystals may be softer, less adhesive, and have less friction (more hydrated or gel-like) than others, depending on how they are formed: by drying or sliding (cf., for example, Figure 5; also compare Figure 6c with Figure 6d).

We used optical transmission microscopy to observe these intentionally dried films, both those that were dried while in contact and those that were dried while separated by a large distance. In either case, several single crystals could be observed over the surfaces (parts b and d of Figure 6). Such single crystals are not found, however, within the contact area of the surfaces that are dried while in contact. The position of the former contact area can be readily identified by a circular region of concentrated dye (Figure 6a). Interestingly, a similar circular region is observed when the surfaces are dried while being separated by a large distance, although this time the concentration of the dye within the circular region is not uniform, being more concentrated near the center and less toward the edge (Figure 6c). The formation of the circular region suggests that two distinct stages may be involved during the evaporation process. When the surfaces are separated by a large distance and allowed to evaporate, the surfaces are initially connected by a large liquid bridge of the solution, which gradually shrinks and then eventually breaks, forming a droplet on each surface. The evaporation rate of the liquid bridge before and after the break may be very different, which could result in the formation of the circular region observed.

Discussion

Perhaps surprisingly, *prior* to crystallization, no significant change in the contrast between the β and γ components of the even-order fringes within the absorption band or in the refractive index of the thin films could be detected under both static and sliding conditions. And since the friction force also remained constant, there is no reason to believe that there was any gradual development of molecular alignment within the shearing film. On the contrary, the onset of crystallization was visually very sudden, and the friction force also remained smooth and steady until crystallization occurred. Moreover, crystallization was accompanied by a dramatic increase in the refractive index and birefringence of the dye film. The process therefore resembles a first-order liquid-to-solid-phase transition, where prior to the nucleation event that leads to freezing there is no change in the short-range order of the liquid molecules. In the present case, however, the freezing or crystallization must be seen as confinement driven (or wall driven) rather than as a bulk phase transition.

BDH^+Cl^- dye is known to crystallize epitaxially on an isolated mica surface,[14] and some of our results can be explained by this epitaxial effect. Formation of several single crystals on the slowly dried surfaces observed by optical microscopy (parts b and d of Figure 6) and the alignment of the dye molecules over a macroscopic area observed via FECO (Figure 5) are consistent with single-surface epitaxial effects. However, a pure epitaxial effect alone cannot account for the crystallization under confinement and shear. Formation of crystals within the contact area takes place much more quickly when the surfaces are confined and sheared than when the surfaces are not confined or confined but kept stationary.

We note that recent studies on freeze-fracture atomic force micrographs of *n*-eicosane films, a few molecular layers thick, between two sliding mica surfaces showed formation of striped domains after prolonged shear of the mica surfaces.[1] Although there was no information as to the orientation of the *n*-eicosane molecules inside each domain (the striped domains were not even parallel to the sliding direction), it was concluded that the formation of the domain structure was induced by shear since control experiments under compression but without shear showed no domain formation. Similarly, Tsai et al.[15] have recently shown that when millimeter-sized colloidal spheres in a semi-bulk liquid of thickness 14−40 layers are subjected to long-term unidirectional shearing, an ordered "crystallized" and a disordered state gradually separate out. The particle density increased gradually over a long time ($\sim 10^4$ s) until crystallization occurred fairly abruptly, similar to what we observed. Crystallization did not occur at very high shear velocities or for thicker film or between smooth but unstructured surfaces.

By consideration of the above two studies together with ours, it appears that crystallization can be induced or suppressed depending on the magnitude of the shear rate and whether the epitaxial interactions are favorable or unfavorable. These effects depend on the number of layers (of molecules or particles) between the confining surfaces and on the shearing direction relative to the surface or lattice structure.

The crystallization of confined dye may be due to the favorable long-range electrostatic interaction with the mica surfaces in water that allows the local concentration to exceed the solubility limit, with the mica surfaces further providing nucleation sites for crystal formation. A pure concentration effect is, however, unlikely: crystallization was observed in films as thick as 20 nm, whereas the increased concentration due to electrostatic interactions is unlikely to extend beyond 1−2 nm. In addition, shear was essential for crystallization to occur within the time scales observed. Even without a large concentration enhancement gradient, shear could lead to local alignment (ordering) of the molecules, thereby triggering nucleation and crystallization. Thus, it is conceivable that the nucleation and crystallization are most likely triggered by a combination of confinement, shear, and epitaxial interactions, i.e., determined by the pressure, the shearing direction, sliding velocity, and the orientation of the confining surface lattices. If so, the crystals may not necessarily nucleate parallel or perpendicular to the shearing direction or to the optic or crystallographic axes of the mica.

Past experimental and theoretical studies[16−19] have suggested that tribological properties generally depend on the subtle details of the sub-nanoscale configuration of the molecules and confining surfaces. In addition, only a small change in the ordering of simple liquids is expected in films on going from static to shearing conditions. Our results are in qualitative agreement with these notions. No big change in alignment of the highly anisotropic dye molecules was observed prior to crystallization in the range of sliding speeds studied. The friction data also showed no significant change (until the surfaces got damaged *after* crystallization). Consequently, our studies show only a weak effect of molecular anisotropy on shear-induced ordering, friction forces, and the onset of shear-induced crystallization, although dramatic changes do occur when the confined molecules are ultimately forced to crystallize.

Acknowledgment. This work was supported by a grant from the U.S. Department of Energy (Grant No. DE-FG03-87ER-45531).

References and Notes

(1) Drummond, C.; Alcantar, N.; Israelachvili, J. N. *Phys. Rev. E* **2002**, *66*, 011705.

(2) Berman, A. D.; Israelachvili, J. N. *Microtribology and Microrheology of Molecularly Thin Liquid Films*; CRC Press: Boca Raton, FL, 2000; Vol. 1.

(3) Berman, A. D. University of California, Santa Barbara, 1996.

(4) Nakatsu, K.; Yoshioka, H.; Morishita, H. *Acta Crystallogr., Sect. B: Struct Sci.* **1977**, *33*, 2181.

(5) Tyutyulkov, N.; Fabian, J.; Mehlhorn, A.; Dietz, F.; Tadjer, A. *POLYMETHINE DYES: Structure and Properties*; St. Kliment Ohridski University Press: Sofia, 1991.

(6) Daehne, L.; Tao, J.; Mao, G. Z. *Langmuir* **1998**, *14*, 565.

(7) Czikkely, V.; Forsterling, H. D.; Kuhn, H. *Chem. Phys. Lett.* **1970**, *6*, 11.

(8) Grunewald, T. Oberflachenkrafte und optische Eigenschaften molekular dunner Schichten, Mainz, 1997.

(9) Alig, A. R. G.; Gourdon, D.; Israelachvili, J. N. in preparation.

(10) Ruths, M.; Granick, S. *Langmuir* **2000**, *16*, 8368.

(11) Briscoe, W. H.; Horn, R. G. Optical phase change at the interface between mica and thin silver film. *J. Opt. A: Pure Appl. Opt.* **2004**, *6*, 112.

(12) Heuberger, M.; Luengo, G.; Israelachvili, J. *Langmuir* **1997**, *13*, 3839.

(13) Israelac. Jn. *J. Colloid Interface Sci.* **1973**, *44*, 259.

(14) Grunewald, T.; Dahne, L.; Helm, C. A. *J. Phys. Chem. B* **1998**, *102*, 4988.

(15) Tsai, J. C.; Gollub, J. P. *Phys. Rev. E* **2004**, *70*.

(16) Yoshizawa, H.; Chen, Y.-L.; Israelachvili, J. *J. Phys. Chem.* **1993**, *97*, 4128.

(17) Maeda, N.; Chen, N. H.; Tirrell, M.; Israelachvili, J. N. *Science* **2002**, *297*, 379.

(18) Gao, J. P.; Luedtke, W. D.; Gourdon, D.; Ruths, M.; Israelachvili, J. N.; Landman, U. *J. Phys. Chem. B* **2004**, *108*, 3410.

(19) Persson, B. N. J. *Sliding friction: physical principles and applications*, 2nd ed.; Springer: Berlin; New York, 2000.